



AUSTRALIAN ATOMIC ENERGY COMMISSION
RESEARCH ESTABLISHMENT
LUCAS HEIGHTS

CALIBRATION OF A JSEM-200 ELECTRON MICROSCOPE

by

R.G. BLAKE

A. JOSTSONS

P.M. KELLY

October 1975

0 642 99716 0

AUSTRALIAN ATOMIC ENERGY COMMISSION
RESEARCH ESTABLISHMENT
LUCAS HEIGHTS

CALIBRATION OF A JSEM-200 ELECTRON MICROSCOPE

by

R.G. BLAKE

A. JOSTSONS

P.M. KELLY

ABSTRACT

The results of a detailed calibration of a JSEM-200 scanning transmission electron microscope are reported. Two types of measurements have been made: (a) calibration of the various parameters associated with scanning transmission (STEM) imaging, and (b) calibration of the usual parameters required for analytical diffraction contrast experiments in the conventional transmission mode (CTEM). The report also contains a detailed discussion of the various STEM imaging modes and the microscope settings necessary to obtain the required image.

National Library of Australia card number and ISBN 0 642 99716 0

The following descriptors have been selected from the INIS Thesaurus to describe the subject content of this report for information retrieval purposes. For further details please refer to IAEA-INIS-12 (INIS: Manual for Indexing) and IAEA-INIS-13 (INIS: Thesaurus) published in Vienna by the International Atomic Energy Agency.

CALIBRATION; ELECTRON DIFFRACTION; ELECTRON MICROSCOPES;
IMAGES; LENSES

CONTENTS

	<u>Page</u>
1. SCANNING TRANSMISSION ELECTRON MICROSCOPE (STEM) FACILITY	1
1.1 Introduction	1
1.2 Calibration Procedure and Results	3
2. CONVENTIONAL TRANSMISSION ELECTRON MICROSCOPE (CTEM)	6
2.1 Introduction	6
2.2 Magnification Calibration	6
2.3 Camera Constant	7
2.4 Rotation Calibration	7
2.5 Precautionary Note	8
3. ACKNOWLEDGMENTS	8
4. REFERENCES	8

- Figure 1 Schematic ray diagrams for (a) conventional transmission electron microscopy (CTEM) and (b) scanning transmission electron microscopy (STEM) showing various beam cone angles and their relationship via the principle of reciprocity.
- Figure 2 Schematic diagram illustrating the angles $2\alpha_i$, $2\alpha_c$ and $2\theta_B$ in relation to a diffraction pattern taken in STEM mode. (After Yamamoto et al. (1974)).
- Figure 3 Condenser/objective lens current combinations for focussed image and diffraction pattern in STEM mode of JSEM-200 operating at 200 kV. The lower curve gives the magnification ratio (with respect to the magnification of the standard position of CL 60 mA / OL 66 mA) as a function of objective lens current.
- Figure 4 Camera constant (λL), camera length L, and relative rotation between image and diffraction pattern — all plotted as a function of objective lens current. STEM mode, 200 kV.
- Figure 5 Variation of illuminating (condenser) aperture angle $2\alpha_i$ and collecting (intermediate) aperture angle $2\alpha_c$ with objective lens current. Curves for a number of different aperture sizes are shown. STEM mode, 200 kV.
- Figure 6 Variation of collecting angle $2\alpha_c$ for objective apertures with objective lens current. STEM mode, 200 kV.

(Continued)

- Figure 7 Curves from Figure 3 showing appearance of the diffraction pattern on the microscope screen at various lens settings. The circular outline of the patterns corresponds to the image of the fixed intermediate aperture (see text for details). STEM mode, 200 kV.
- Figure 8 Magnification calibration for 200 kV as a function of magnification meter reading. CTEM mode.
- Figure 9 The relationship between objective lens and magnification meter readings at selected magnifications for Range 3 at 200 kV. CTEM mode.
- Figure 10 Variation of camera constant, λL , with objective lens 'current' for S.A.D. 1 position at 200 kV. Camera constant for S.A.D. 2 position can be obtained by multiplying the relevant S.A.D. 1 value with 0.5822. CTEM mode.
- Figure 11 Relative rotation of the image with respect to the diffraction pattern (at S.A.D. 1) as a function of magnification meter reading and accelerating voltage for Ranges 1 and 2. CTEM mode, 200 kV.
- Figure 12 Relative rotation of the image with respect to the diffraction pattern (at S.A.D. 1) as a function of magnification meter reading and accelerating voltage for Range 3. CTEM mode, 200 kV.

1. SCANNING TRANSMISSION ELECTRON MICROSCOPE (STEM) FACILITY

1.1 Introduction

Commercial electron microscopes fitted with attachments for scanning transmission electron microscopy (STEM) have become available in the last two to three years. By comparison with conventional transmission electron microscopes (CTEM), a number of advantages are claimed for these new instruments — greater penetration, electronic image processing, less chromatic aberration, and microdiffraction capabilities.

Image formation in STEM is related to CTEM through the principle of reciprocity (Cowley 1969) and, for equivalent beam cone angles, identical images are produced in both modes. When STEM images differ from CTEM images, this is invariably related to differences in the beam divergence angles (Brooker et al. 1974; Yamamoto et al. 1974). In CTEM, the cone angle of the incident beam is limited by the need to illuminate the area of specimen uniformly, while the useful acceptance angle of the objective lens is limited by lens aberrations. In STEM however, there are fewer restrictions on the equivalent angles. The detector acceptance angle $2\alpha_c$, which by reciprocity is equivalent to the illumination beam angle in CTEM, can be varied by means of a selector aperture between the specimen and the detector (Figure 1). This does not adversely affect the image resolution and any loss in brightness of the image, caused by a reduction in acceptance angle, can be electronically compensated on the video display. The STEM beam illuminating angle $2\alpha_i$ — the equivalent of the objective aperture acceptance angle in CTEM — can be varied by altering the condenser aperture (Figure 1). This leads to a deterioration in resolution with increase in condenser aperture size.

Another method of controlling the illuminating angle $2\alpha_i$ is to change the condenser/objective lens current combinations required to form a focussed probe on the specimen. This also results in a loss of resolution as the selected current combination departs from the ideal for the lenses on the instrument. However, the condenser/objective lens current combination method allows variations in $2\alpha_i$ over a very wide range — from 10^{-3} to 5×10^{-2} radians.

In the materials science field, the advantages conferred by the ability to control $2\alpha_i$ and $2\alpha_c$ have been outlined by Yamamoto et al (1974). Obviously these advantages must be utilised to the fullest extent and it is pointless employing STEM, with a resolution of say 2 nm, to duplicate images that can

easily be obtained in CTEM, with a resolution of better than 0.5 nm. The most relevant information likely to emerge from STEM instruments will almost certainly come from experiments conducted under conditions widely different from those used for CTEM. The calibration of the STEM facility of the JSEM-200 at the AAEC Research Establishment, Lucas Heights, was carried out with this principle in mind. As a result, the widest possible range of image-forming conditions were investigated, and every attempt was made to depart from the standard lens settings recommended in the Instruction Manual*.

Some of the more important parameters measured are given in Figure 2, which is a slight simplification of the equivalent diagram used by Yamamoto et al. (1974). Essentially, the unique features of STEM images are associated with the relative values of $2\alpha_i$, $2\alpha_c$ and $2\theta_B$. Following Yamamoto et al., but modifying their abbreviations slightly, a number of distinct situations exist. These are:

- . Single or separate illumination (SI) where $2\alpha_i < 2\theta_B$ and there is no overlap between transmitted and diffracted beams.
- . Mixed illumination (MI) where $2\alpha_i > 3$ to $4\theta_B$ and the transmitted and diffracted beams overlap to a significant extent.
- . Single-beam imaging (SBI) where $2\alpha_c < 2\theta_B$. This is the nearest equivalent to CTEM imaging and is only possible under conditions of separate illumination.
- . Multi-beam imaging (Hashimoto et al. 1974) (MBI) where $2\alpha_c > 2\theta_B$ and in general $2\alpha_c$ is 3 to $4\theta_B$. This can obviously be done under separate or mixed illumination.

These distinct illumination and collection regimes can be combined in a number of ways, i.e. SI/SBI, SI/MBI and MI/MBI. As mentioned above, SI/SBI is the equivalent of CTEM provided $2\alpha_c$ and $2\alpha_i$ are kept small. If $2\alpha_i$ is fixed to give separate illumination and $2\alpha_c$ is increased, dynamic effects such as thickness fringes, bend contours and, to a lesser extent, stacking fault fringes begin to blur and eventually disappear (Brooker et al. 1974; Yamamoto et al. 1974). This increase in the collector angle $2\alpha_c$ eventually leads to the formation of a multi-beam image (SI/MBI) with very little in

* Instruction Manual - JSEM-200 (1974). Japan Electron Optics Laboratory Ltd., Tokyo, Japan.

the way of conventional, dynamic contrast. The third combination — MI/MBI — is also free of dynamic effects, but has the additional advantage that bands of high anomalous absorption are eliminated when the overlap of incident and diffracted beam is considerable.

1.2 Calibration Procedure and Results

The above discussion gives some of the changes to be expected by varying $2\alpha_i$ and $2\alpha_c$. In the JSEM-200, quite a wide range of these two angles is possible via appropriate selection of the condenser (CL) and objective (OL) lens current combination required to form an image. All STEM calibrations were done at 200 kV and, where appropriate, were referred to the standard image position of CL 60 mA / OL 66 mA. This standard setting plus all other settings described below depend, to some extent, on specimen position as determined by the Z control of the side-entry goniometer. In all cases, Z was adjusted for optimum tilting i.e. specimen in a plane containing one tilt axis.

The possible condenser/objective lens current combinations were determined by varying the objective lens current (usually in 1 mA steps) and then adjusting the condenser lens current to give a focussed image. As Figure 3 shows, this leads to a double-branched curve with the standard position CL 60 mA / OL 66 mA at the extreme of one branch. Movement along this branch towards CL 46 mA / OL 72 mA was accompanied by a progressive decrease in resolution. The position on the opposite branch corresponding to the standard setting was CL 25 mA / OL 65 mA; from limited resolution tests this appeared to be almost as good as the standard setting. As the lens currents were altered along this lower branch towards CL 44 mA / OL 58 mA, a similar deterioration in resolution was observed. There was a progressive change in magnification from OL 58 mA to OL 72 mA. This is represented as a ratio of magnification at a given objective setting to magnification at the standard objective current setting which corresponds to the value on the direct reading magnification meter on the STEM console. These values are plotted as a function of objective lens current at the bottom of Figure 3.

For each image position, the diffraction pattern on the screen was observed and, with the objective lens current kept constant, the condenser lens was varied until the diffraction pattern appeared fully focussed. These lens settings are also included in Figure 4. The focussing of the diffraction pattern with the condenser lens had no effect on the camera

length or angle of the pattern on the screen; however, changing the objective lens current led to a change in camera length and a rotation of the diffraction pattern. This is shown in Figure 4 along with the image rotation caused by the change in objective lens current and the total angle between image on the cathode-ray tube and the diffraction pattern.

The values of the angles $2\alpha_i$ and $2\alpha_c$ were determined by taking diffraction patterns of aluminium with the conventional microscope plate camera. All the results are for patterns taken at the lens settings corresponding to a focussed image. The $\{200\}$ and $\{311\}$ spacings of aluminium were used to relate distances to angles on the plate. Figure 5 shows the variation of illumination angle $2\alpha_i$ as a function of objective lens current. Most determinations were made with a $70\ \mu\text{m}$ diameter condenser aperture. The value of $2\alpha_i$ is directly proportional to the condenser aperture diameter so that, apart from a few check values measured with the $200\ \mu\text{m}$ aperture, the curves for the other condenser aperture sizes have been plotted as simple ratios of the $70\ \mu\text{m}$ master curve.

Figure 5 shows the very large variation in $2\alpha_i$ that is possible; note that the angle is plotted on a logarithmic scale. Also shown on Figure 5 is the collection angle $2\alpha_c$ as a function of objective lens current for the fixed 6-mm diameter intermediate aperture and two of the variable intermediate apertures. This collection angle decreases with objective lens current and at low values of this current the maximum amount of the diffraction pattern is visible on the screen. This corresponds to the variation in camera length shown in Figure 4.

The same procedure was adopted to determine the collection angle $2\alpha_c$ for various objective apertures, and this is shown in Figure 6. As was the case with the intermediate apertures, the value of $2\alpha_c$ is directly proportional to aperture diameter, so only one aperture was measured and the corresponding values for other aperture sizes plotted as simple ratios. By making use of both objective and intermediate apertures, a fairly comprehensive range of $2\alpha_c$ values is possible at any given objective lens setting.

A pictorial representation of some of the information given graphically in Figure 5, is shown in Figure 7. The points to note on this figure are:

- . The circles outlining the diffraction patterns represent the image of the fixed 6-mm diameter intermediate aperture and so correspond to $2\alpha_c$ for this aperture.
- . The image of the 1-mm variable intermediate aperture has been double exposed onto the centre spot of the pattern. In most cases, the discrete circle corresponding to this image is swamped by the high intensity associated with the centre spot, but it is clearly visible in the patterns corresponding to CL 35 mA / OL 64.5 mA and CL 60 mA / OL 66 mA.
- . Because of the change in λL (or $2\alpha_c$) with objective lens current more of the diffraction pattern is visible at low objective lens current positions.
- . With a 70 μm diameter condenser aperture, mixed illumination (MI) can be obtained at objective lens currents in the range 64 to 66.5 mA. Note - images cannot be formed between 65 and 66 mA objective lens current.
- . Microdiffraction with selected areas of 100 to 200 \AA diameter is best carried out when the focussed image curve approaches the focussed diffraction pattern curve. This gives the best "spot" pattern even when the lenses are set for focussed image. Changing the condenser lens setting to the value corresponding to a focussed diffraction pattern greatly increases the area of specimen covered by the probe, so for true microdiffraction the pattern must be recorded with the focussed image setting. This means that there are essentially two positions where microdiffraction is possible. The first of these is at OL lens settings of 70 to 72 mA and the second is on the other branch of the curve at OL lens settings of 60 to 62 mA. The former is the position recommended in the Instruction Manual (CL 46 mA / OL 72 mA). However, the Manual makes no mention of the second branch of the curve, and microdiffraction at CL 43 mA / OL 60 mA has the additional advantage of allowing more of the diffraction spots to be recorded on the screen (smaller λL).
- . The Kikuchi lines are always more pronounced and easily visible in diffraction patterns at the focussed image settings.

2. CONVENTIONAL TRANSMISSION ELECTRON MICROSCOPE (CTEM)

2.1 Introduction

Results are presented of calibration measurements on the AAEC JSEM-200 electron microscope at Lucas Heights. The calibration consists of three sets of measurements:

- . Magnification as a function of meter reading and objective lens current.
- . Camera constant and its dependence on objective lens current.
- . Relative rotations between the image and selected area diffraction pattern as a function of magnification meter reading.

The various lens currents on the JSEM-200 are displayed on a milliammeter via a selector switch. A parallax effect limits the accuracy of reading to about 1 mA. It was found convenient to incorporate a digital voltmeter in the measuring circuit; consequently although the following discussion is concerned mainly with lens currents, the actual readings in the calibration are measurements of the voltage across the shunt of the milliammeter. The relationship between the ammeter current and the digital voltmeter reading is $1 \text{ mA} \equiv 2 \text{ mV}$.

The calibrations were carried out using the double-tilt ($\pm 45^\circ$) side-entry goniometer which is equipped with a height adjustment (termed Z control) to permit the specimen plane to be made coincident with the tilting axis; this is called the $Z = 0$ position.

2.2 Magnification Calibration

There are three magnification ranges on the JSEM-200. The magnification is mainly a function of intermediate lens current on ranges M2 and M3 where the projector lens current is fixed at maximum, and projector lens current on range M1 where the intermediate lens current is not variable. The calibration was carried out only at 200 kV using a replicated grating with a spacing of 2160 lines per mm. At high magnification, where the line spacing exceeded the plate width, a suitable fine irregularity on the replica was used for measurement.

Effects of objective lens current were investigated only for range M3 at 200 kV. Variations in objective lens current were achieved by raising or lowering the specimen via the Z control. The three levels of objective current investigated correspond to $Z = 0$ and Z at maximum and minimum heights.

Results are plotted in Figure 8 and currents for selected magnifications at 200 kV, obtained by interpolation, are shown in Figure 9.

2.3 Camera Constant

For small diffraction angles, Bragg Law can be written as

$$Rd = \lambda L \quad , \quad \dots(1)$$

where R is the radial distance between the diffraction spot and the zero order spot, d is the interplanar spacing, λ is the electron wave length and L is the distance between the specimen and the photographic plate.

The camera constant, λL , was determined as a function of objective lens current at 200 kV (Figure 10) from measurements of R on diffraction patterns from an evaporated, fine grained nickel film ($a = 3.524 \text{ \AA}$). These measurements were made at the S.A.D. 1 position*. One measurement was also made at the S.A.D. 2 position from which values at other objective lens current settings can be derived.

Values of λL for other accelerating voltages can be derived by the equation

$$(\lambda L)_{kV} = (\lambda L)_{200} \cdot \frac{(\lambda)_{kV}}{(\lambda)_{200}} \quad \dots(2)$$

Unfortunately, the objective lens currents change with accelerating voltage, hence the calibration curve is not directly applicable at voltages other than 200 kV with the important exception of the $Z = 0$ position (see Figure 10).

2.4 Rotation Calibration

Before crystallographic directions, determined from the diffraction pattern, can be assigned to the image, the image and diffraction pattern must be made coincident by correcting for rotations due to lens magnetic fields. The rotations as a function of lens current were determined using a set of (001) θ' plates in an Al-Cu alloy imaged under two beam $g = 200$ conditions. The results are shown in Figures 4 and 5 and include the 180° Groves and Whelan (1962) inversion which was determined by the method described by Head et al. (1973).

The measurements refer to photographic plates viewed with the emulsion side up. To avoid any ambiguity, the relationship between diffraction pattern and the image is shown pictorially in Figures 11 and 12 with a symbol having one-fold rotational symmetry.

* S.A.D. = Selected Area Diffraction

2.5 Precautionary Note

The calibration measurements correspond to a jack current of 53.3 μ A in the reference battery box. We have found that the calibration values can change by as much as 30 per cent with deterioration of the Mallory (101.1 V) reference batteries. To obtain reproducible results, this current must be checked periodically and the battery replaced at the first sign of deterioration.

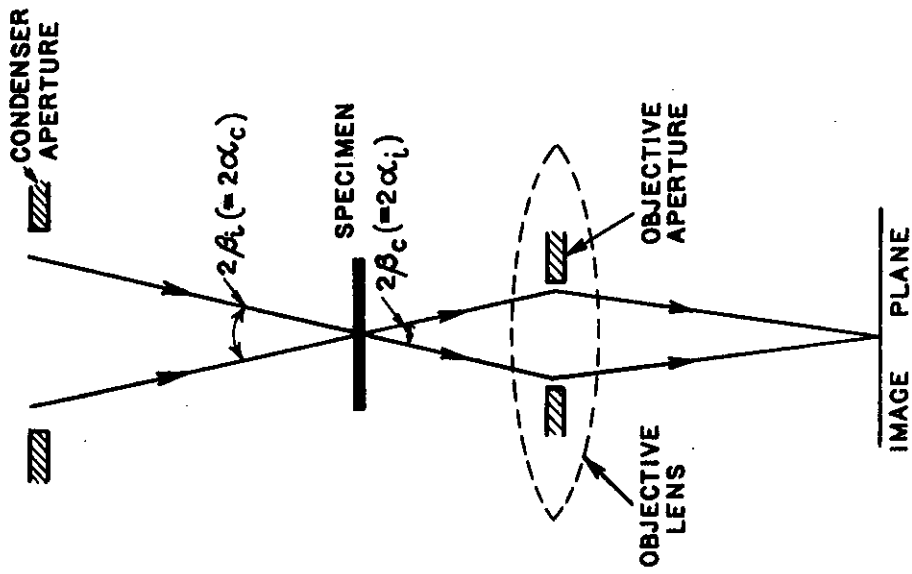
3. ACKNOWLEDGMENTS

The authors would like to thank Dr. N. Morimura of Japan Electron Optics Laboratory for his very considerable time and patience in teaching us the mysteries of STEM microscopy and for making us aware of the alternative microdiffraction position at CL 43 mA / OL 60 mA. The authors are also indebted to Dr. T. Yamamoto of JEOL for very helpful discussions on the use of STEM and for sending us advance copies of his own work on STEM calibration.

4. REFERENCES

- Brooker, G.R., Joy, D.C., Spencer, J.P. and Graf von Harrach, H. (1974) - Scanning Electron Microscopy (11TR1), Chicago, p.226.
- Cowley, J.M. (1969) - Appl. Phys. Lett. 15: 58.
- Groves, G.W. and Whelan, M.J. (1962) - Phil. Mag. 7: 1603.
- Hashimoto, H., Endoh, H., Kumao, A., Shiraishi, K. and Nishigori, N. (1974) - Proc. Int. Crystallography Conf., Melbourne, p.341.
- Head, A.K., Humble, P., Clareborough, L.M., Morton, A.J. and Forwood, C.T. (1973) - Computed Electron Micrographs and Defect Identification. North Holland, Amsterdam, p.43.
- Yamamoto, T., Nishizawa, H. and Shibatomi, K. (1974) - 8th Int. Congr. on Electron Microscopy, Canberra, 1: p.286 (also Yamamoto, T. and Nishizawa, H., (1974) - JEOL News 12e (2) 19).

(a) CTEM



(b) STEM

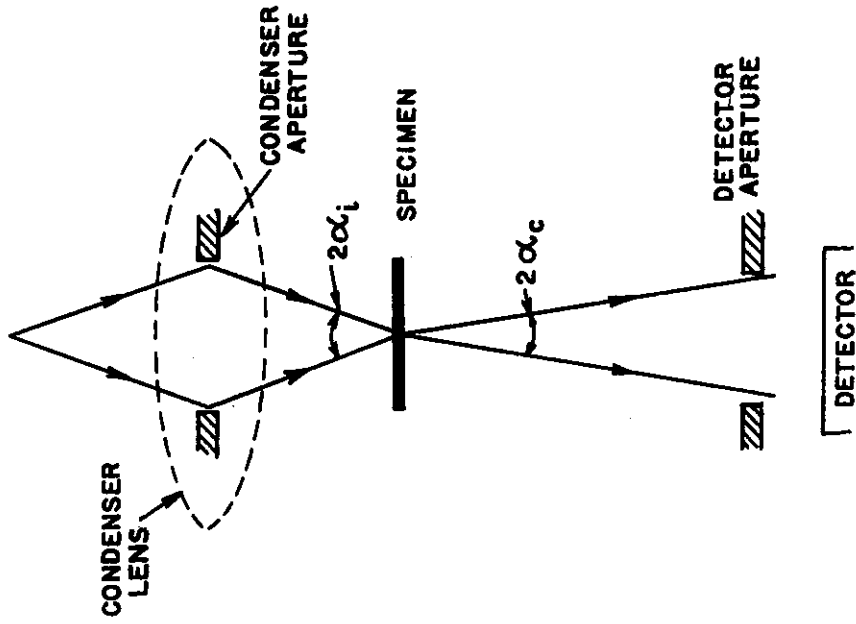
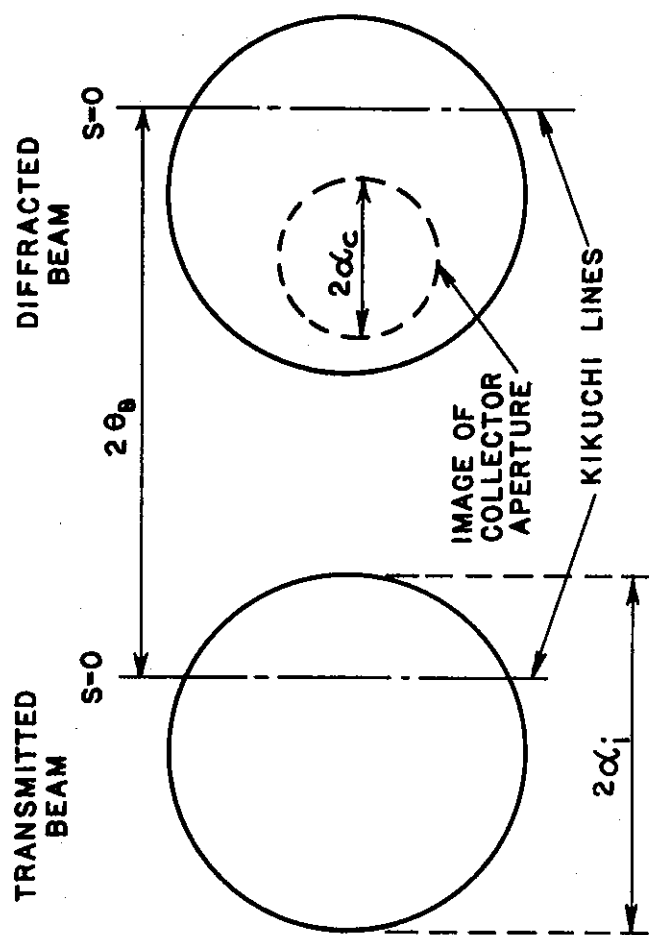


FIGURE 1. SCHEMATIC RAY DIAGRAMS FOR (a) CONVENTIONAL TRANSMISSION ELECTRON MICROSCOPY (CTEM) AND (b) SCANNING TRANSMISSION ELECTRON MICROSCOPY (STEM) SHOWING VARIOUS BEAM CONE ANGLES AND THEIR RELATIONSHIP VIA THE PRINCIPLE OF RECIPROCITY



$2\alpha_i$ = ILLUMINATING ANGLE

$2\alpha_c$ = COLLECTING ANGLE

$2\theta_B$ = TWICE BRAGG ANGLE

FIGURE 2. SCHEMATIC DIAGRAM ILLUSTRATING THE ANGLES $2\alpha_i$, $2\alpha_c$ AND $2\theta_B$ IN RELATION TO A DIFFRACTION PATTERN TAKEN IN STEM MODE (After Yamamoto et al (1974))

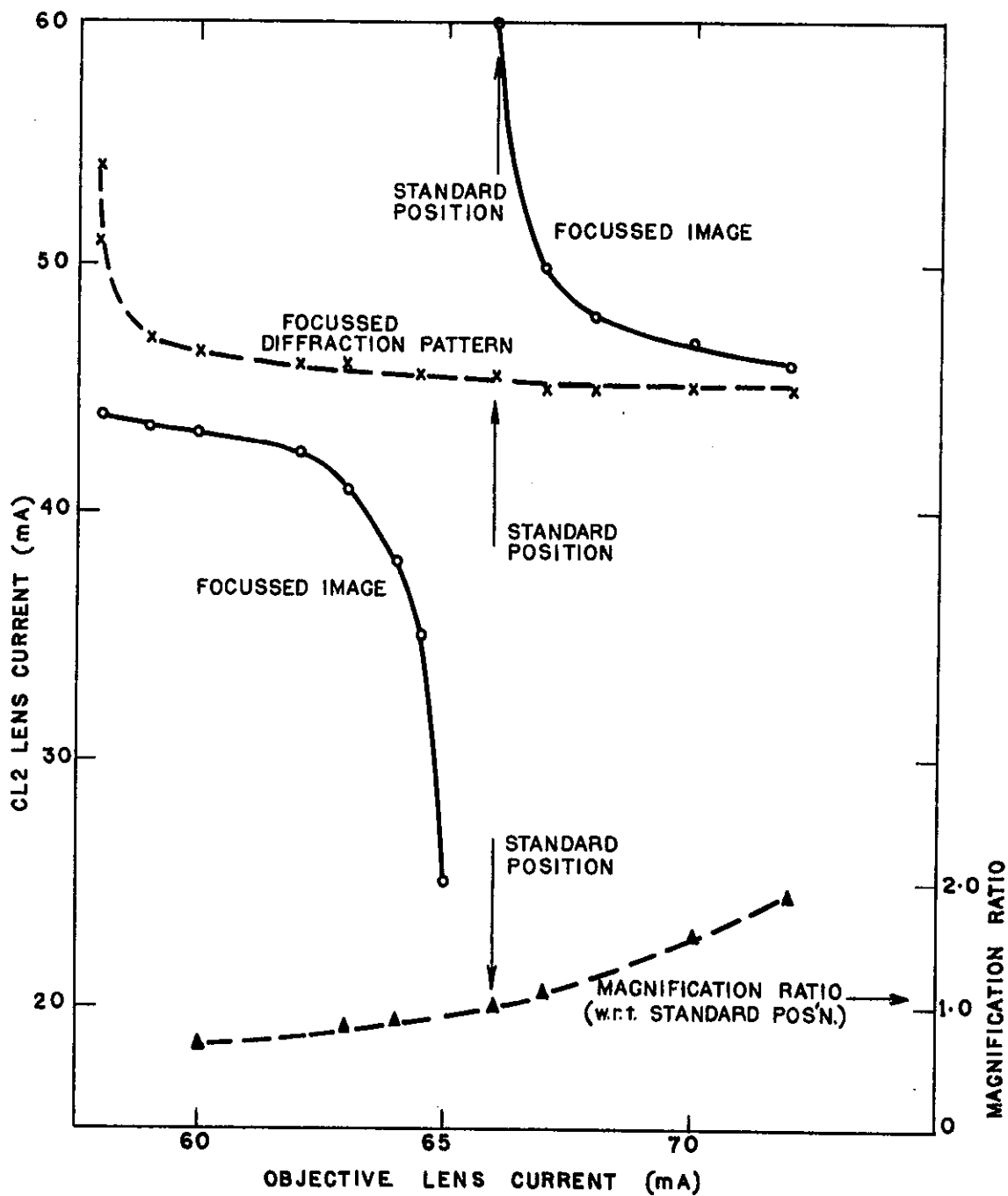


FIGURE 3. CONDENSER/OBJECTIVE LENS CURRENT COMBINATIONS FOR FOCUSED IMAGE AND DIFFRACTION PATTERN IN STEM MODE OF JSEM-200 OPERATING AT 200 kV. THE LOWER CURVE GIVES THE MAGNIFICATION RATIO (WITH RESPECT TO THE MAGNIFICATION OF THE STANDARD POSITION OF CL 60 mA / OL 66 mA) AS A FUNCTION OF OBJECTIVE LENS CURRENT

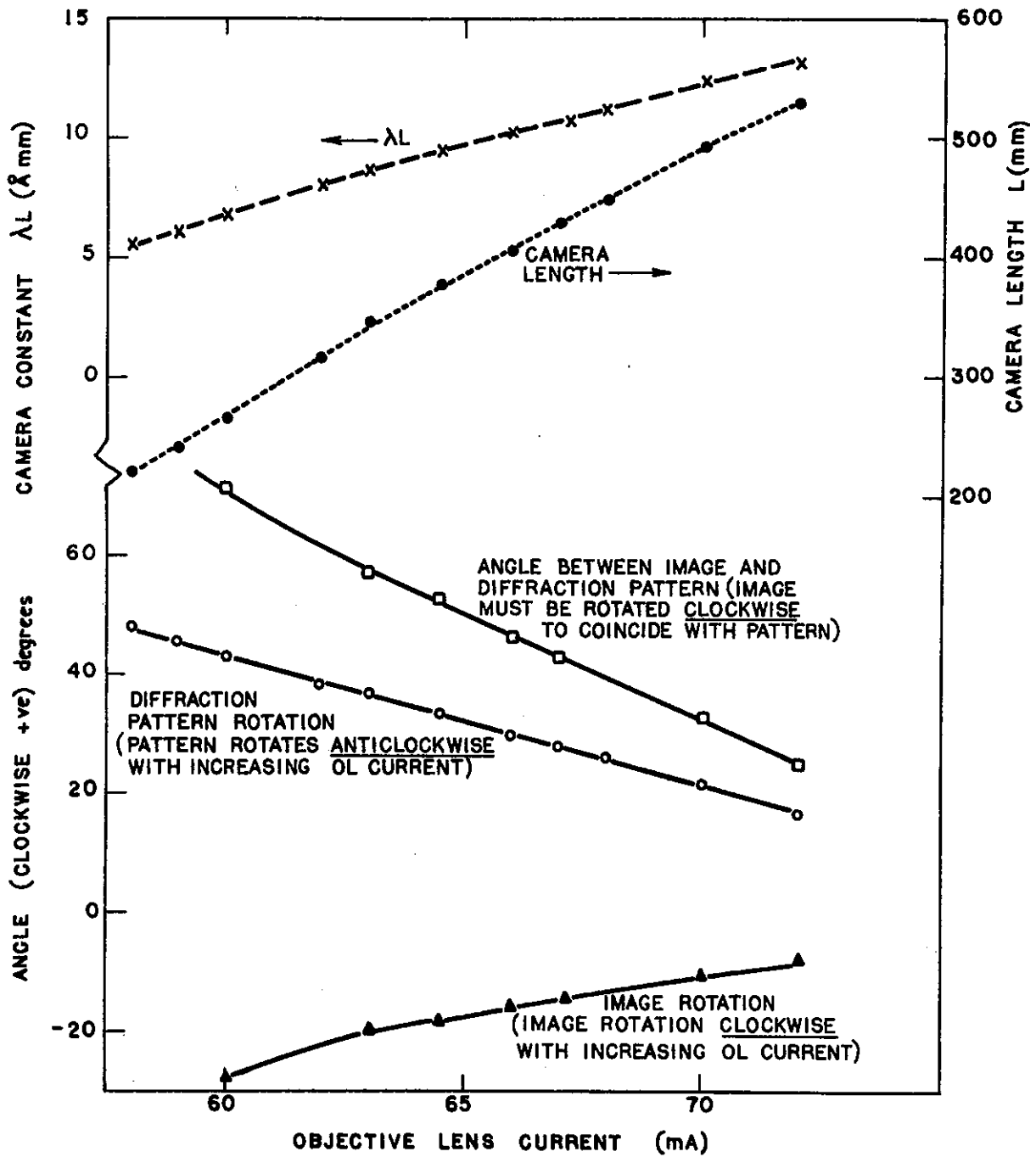


FIGURE 4. CAMERA CONSTANT (λL), CAMERA LENGTH L , AND RELATIVE ROTATION BETWEEN IMAGE AND DIFFRACTION PATTERN - ALL PLOTTED AS A FUNCTION OF OBJECTIVE LENS CURRENT. STEM MODE, 200 kV

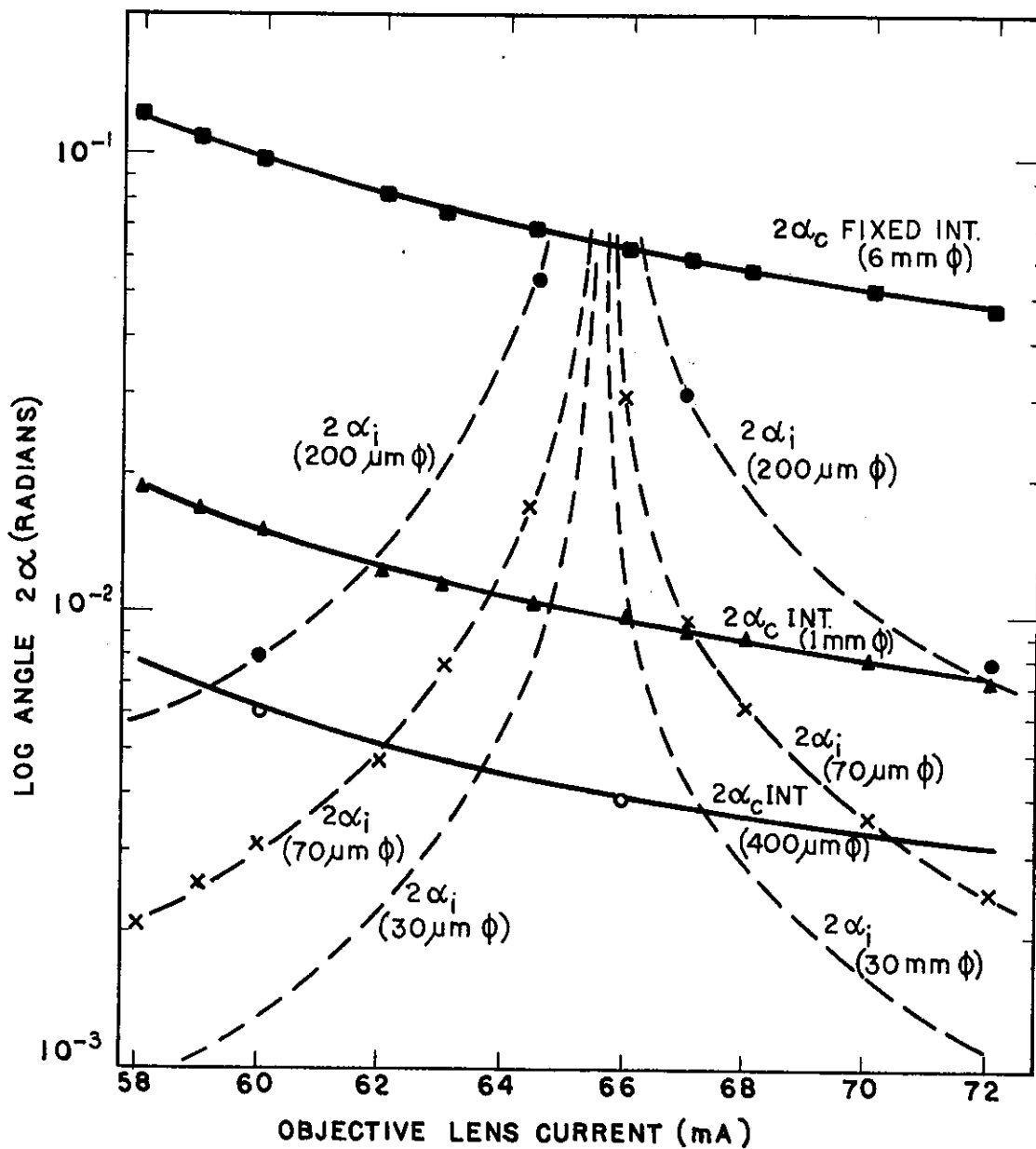


FIGURE 5. VARIATION OF ILLUMINATING (CONDENSER) APERTURE ANGLE $2\alpha_i$ AND COLLECTING (INTERMEDIATE) APERTURE ANGLE $2\alpha_c$ WITH OBJECTIVE LENS CURRENT. CURVES FOR A NUMBER OF DIFFERENT APERTURE SIZES ARE SHOWN. STEM MODE, 200 kV

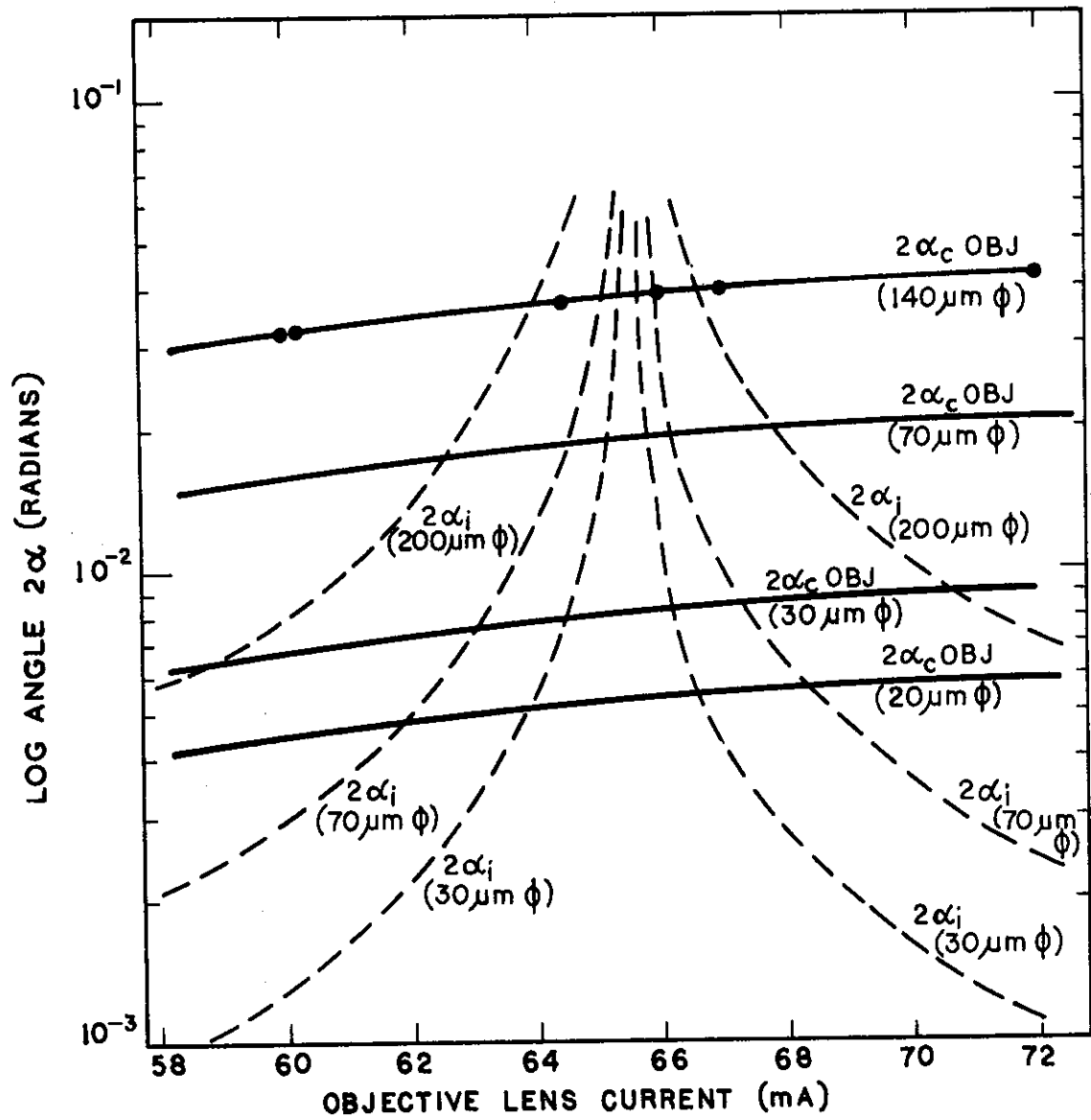
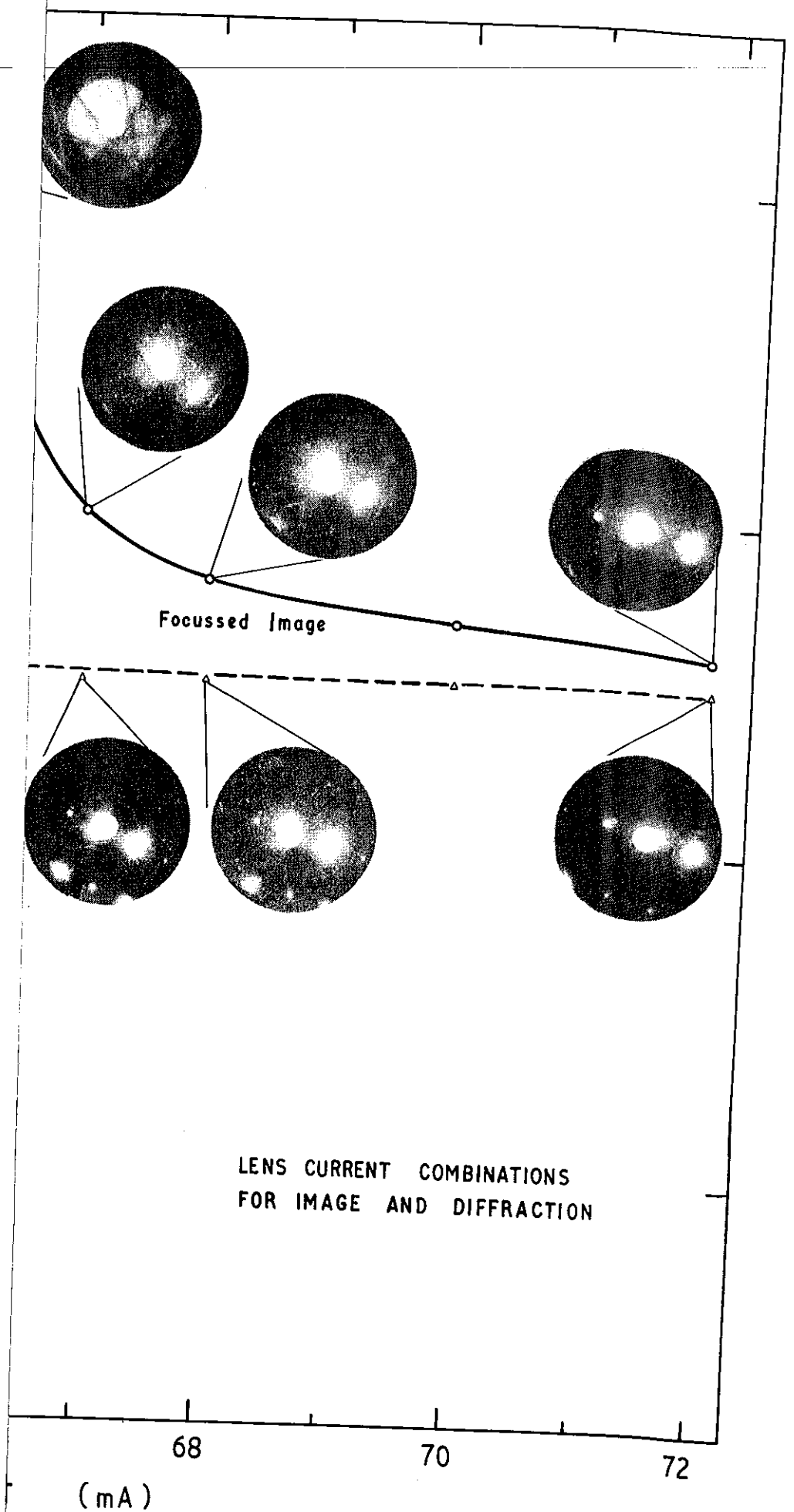


FIGURE 6. VARIATION OF COLLECTING ANGLE $2\alpha_c$ FOR OBJECTIVE APERTURES WITH OBJECTIVE LENS CURRENT. STEM MODE, 200 kV



DIFFRACTION PATTERN ON THE MICROSCOPE SCREEN AT
LENS CURRENTS CORRESPONDS TO THE IMAGE OF THE
OBJECT, 200 kV

FI

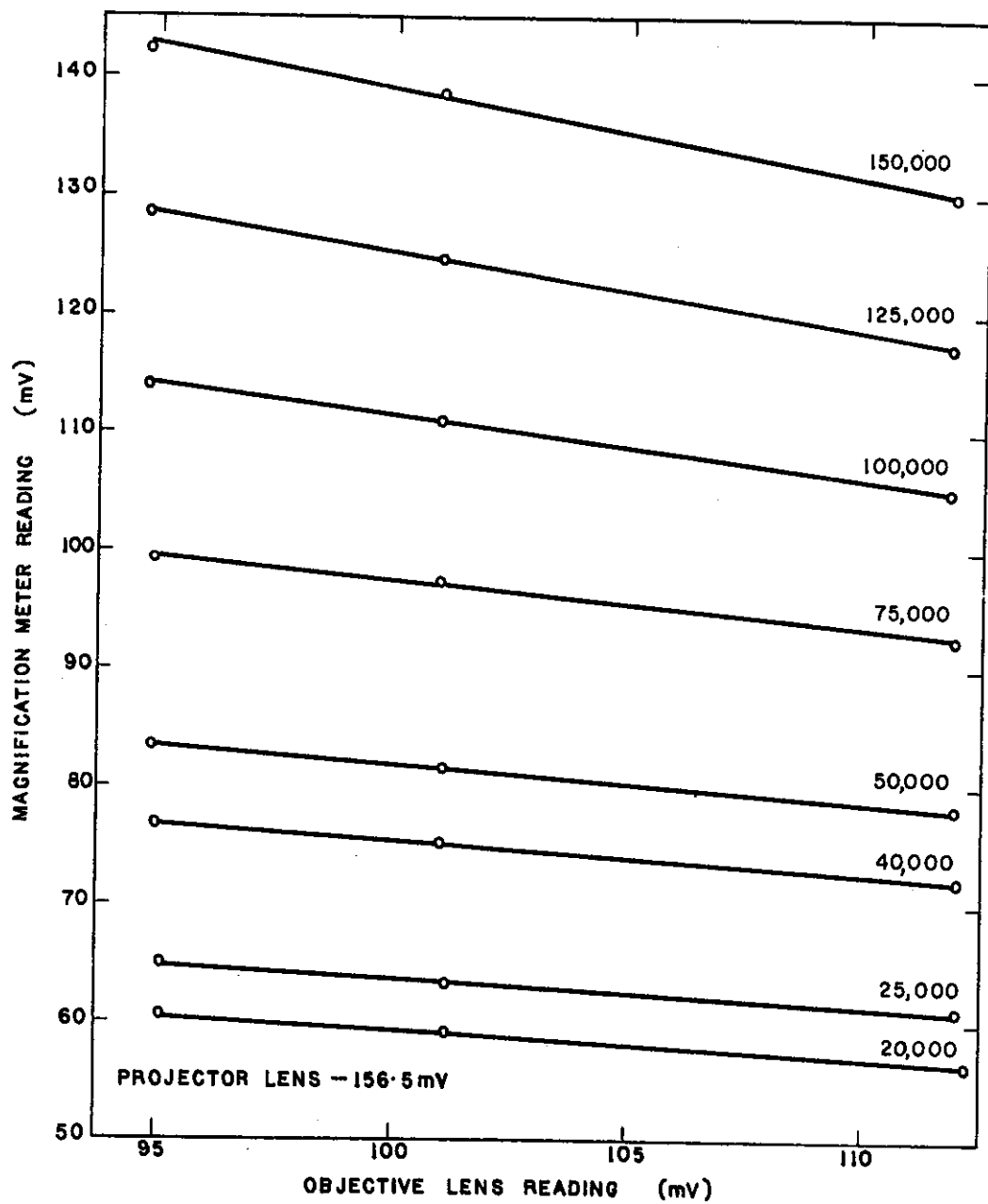


FIGURE 9. THE RELATIONSHIP BETWEEN OBJECTIVE LENS AND MAGNIFICATION METER READINGS AT SELECTED MAGNIFICATIONS FOR RANGE 3 AT 200 kV. CTEM MODE

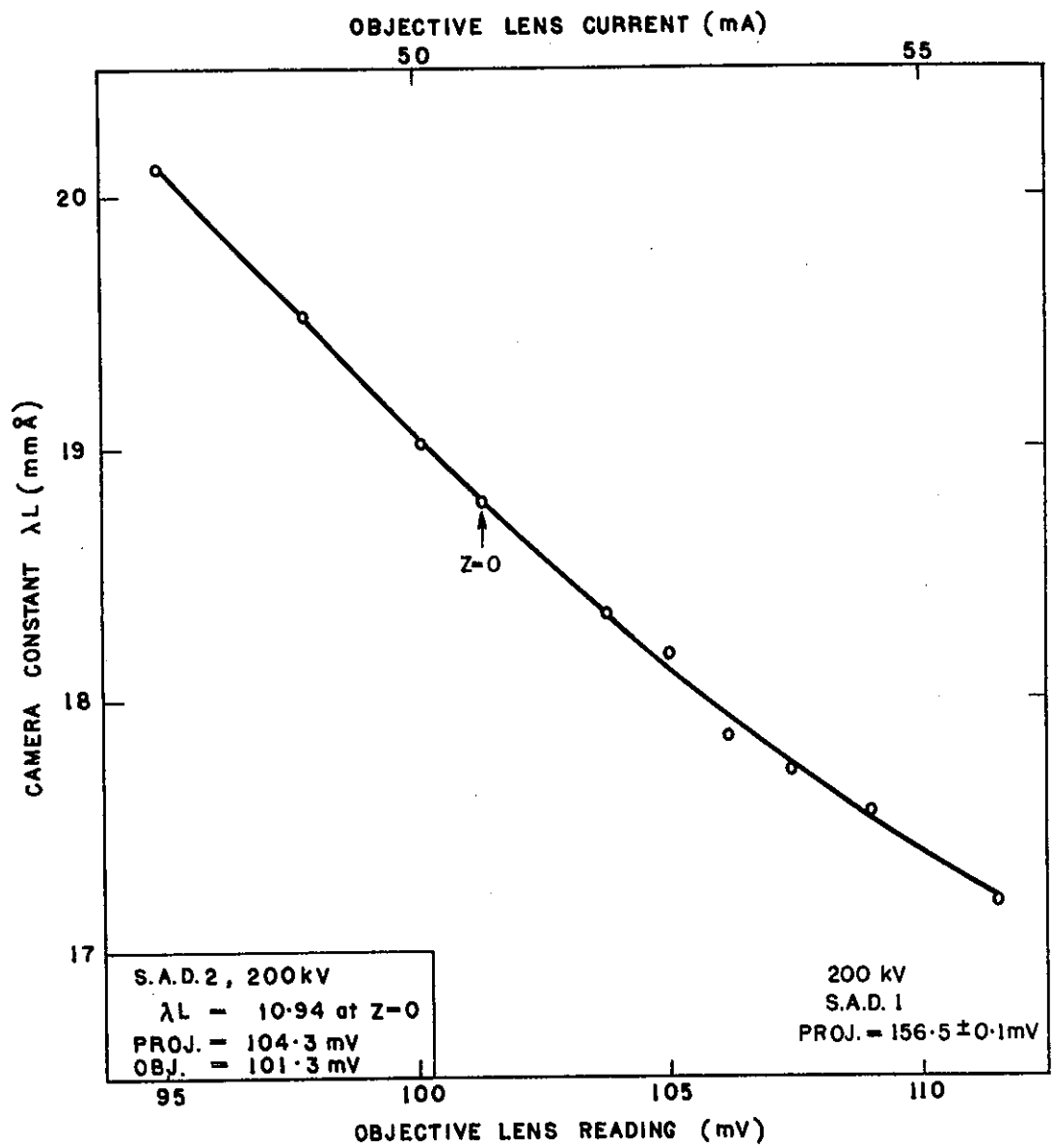


FIGURE 10. VARIATION OF CAMERA CONSTANT, λL , WITH OBJECTIVE LENS 'CURRENT' FOR S.A.D. 1 POSITION AT 200 kV. CAMERA CONSTANT FOR S.A.D. 2 POSITION CAN BE OBTAINED BY MULTIPLYING THE RELEVANT S.A.D. 1 VALUE WITH 0.5822. CTEM MODE

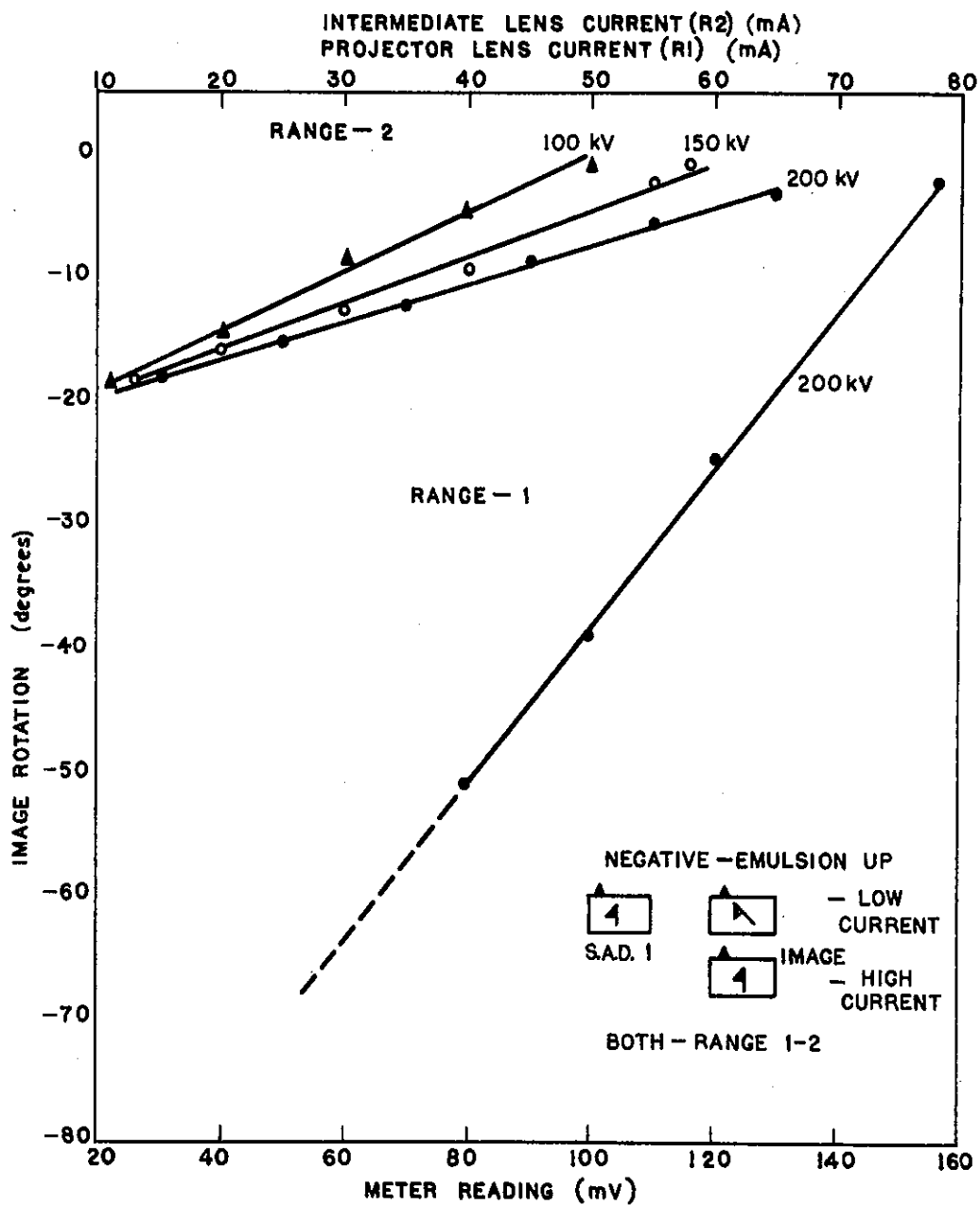


FIGURE 11. RELATIVE ROTATION OF THE IMAGE WITH RESPECT TO THE DIFFRACTION PATTERN (AT S.A.D. 1) AS A FUNCTION OF MAGNIFICATION METER READING AND ACCELERATING VOLTAGE FOR RANGES 1 AND 2. CTEM MODE, 200 kV

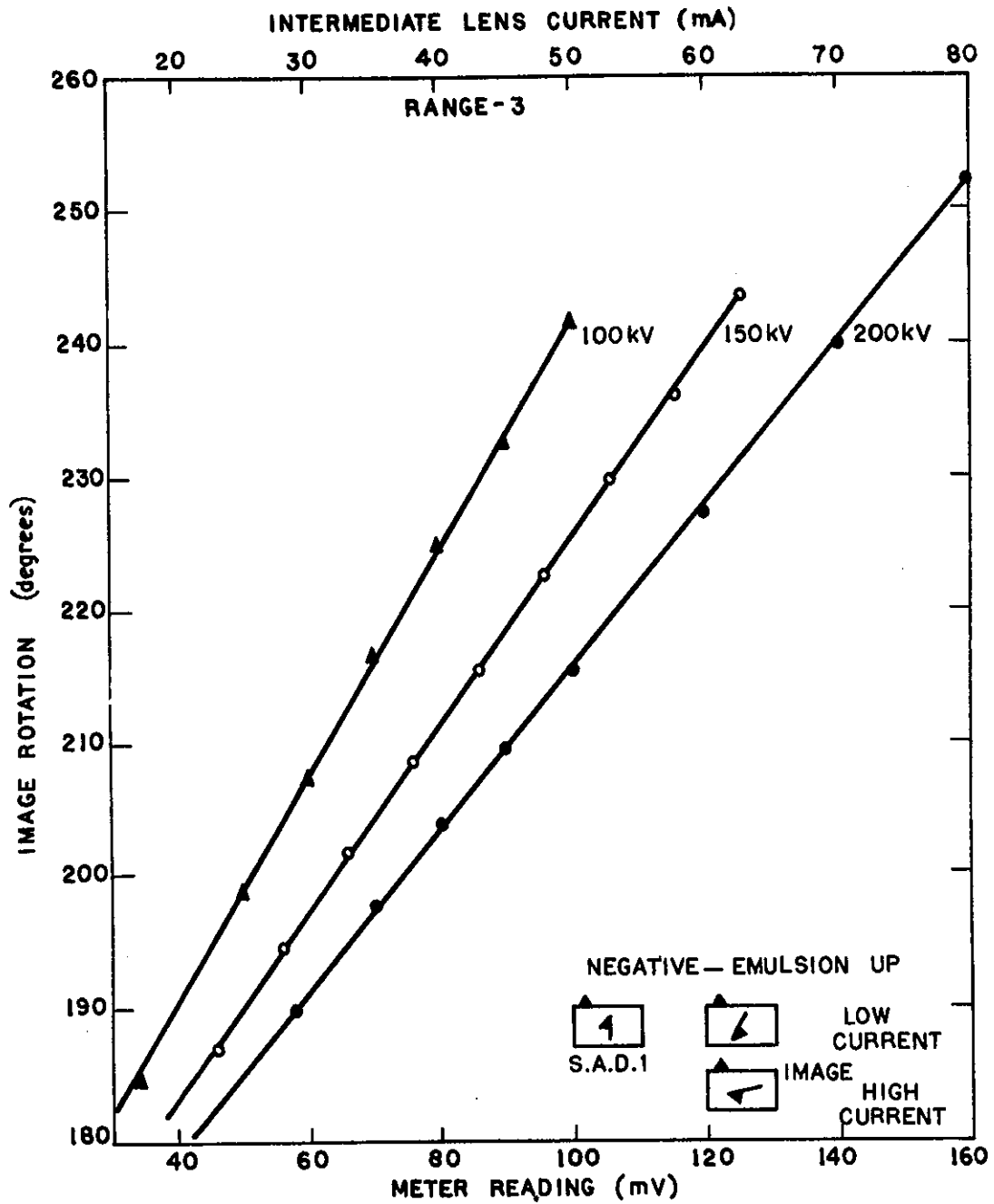


FIGURE 12. RELATIVE ROTATION OF THE IMAGE WITH RESPECT TO THE DIFFRACTION PATTERN AT (S.A.D. 1) AS A FUNCTION OF MAGNIFICATION METER READING AND ACCELERATING VOLTAGE FOR RANGE 3. CTEM MODE, 200 kV